HAL
open science

SEM Characterization of Hydrogenated Nickel

S.S.M. Tavares, A. Lafuente, S. Miraglia, D. Fruchart, B. Lambert, Sébastien Pairis

To cite this version:

S.S.M. Tavares, A. Lafuente, S. Miraglia, D. Fruchart, B. Lambert, et al.. SEM Characterization of Hydrogenated Nickel. Acta Microscopica, 2003, 12 (1), pp.195-198. hal-03607563

HAL Id: hal-03607563

https://hal.science/hal-03607563v1

Submitted on 14 Mar 2022

HAL is a multi-disciplinary open access archive for the deposit and dissemination of scientific research documents, whether they are published or not. The documents may come from teaching and research institutions in France or abroad, or from public or private research centers.

L'archive ouverte pluridisciplinaire **HAL**, est destinée au dépôt et à la diffusion de documents scientifiques de niveau recherche, publiés ou non, émanant des établissements d'enseignement et de recherche français ou étrangers, des laboratoires publics ou privés.

ARTICLE

SEM Characterization of Hydrogenated Nickel

[a,b]S.S.M. Tavares; [c]A. Lafuente; [a]S. Miraglia; [a]D. Fruchart; [a]B. Lambert and [a]S. Pairis
[a]CNRS / Laboratoire de Cristallographie - BP 166, 38042, Grenoble Cedex, France
[b]UFF – Departamento de Eng. Mecânica - Rua Passo da Patria, 156 - 24210-210, Niteroi/RJ, Brazil.
[c] Inst. de Ciências de los Materiales de Aragon, CSIC-Universidad de Zaragoza, 50009, Spain.

Abstract

The effects of hydrogen insertion by electrolytic charging in pure nickel were investigated by scanning electron microscopy (SEM) and X-ray diffraction. The hydrogenated samples (thin foils of 0,02mm) contained at least 50% of $NiH_{0,68}$ hydride just after charging. The $NiH_{0,68}$ hydride and the α-Ni phase were distinguished by scanning electron microscopy (SEM) operating in the backscattered electrons mode. The difference of density or average atomic number between the two phases was enough to obtain a contrast between them. The instability of the nickel hydride at room temperature was observed by X-ray diffraction and by SEM. Interesting features about the intergranular cracks developed during and after charging are discussed.

Introduction

The insertion of hydrogen in metals promotes severe modifications of physical and mechanical properties. In the case of nickel, hydrogen induces intergranular cracking [1], decrease of ferromagnetism [2] and vacancy generation [3]. Large amounts of the fcc β hydride may be produced by high pressure hydrogenation [4] or electrolytic charging [5]. The H/Ni ratio (x) in the β hydride ranges from 0.6 to 1.0, depending on the method and conditions of hydrogenation. The β hydride is known to be metastable at room temperature and normal pressure [6].

For x=H/Ni≤1 the hydrogen atoms occupy the octahedral interstices of the fcc structure promoting cell expansion. As a consequence, the hydride formation must induce compressive stresses. The hydride decomposition (outgassing), however, causes the contraction of the unit cell and tension stresses generation. Tsukuda et al. [7] confirmed experimentally such behaviour in hydrogenated and outgassed palladium.

The stresses developed during outgassing usualy promote delayed cracks in ductile fcc metals. This effect has been observed by many authors in cathodically hydrogenated stainless steels [8-11].

In the present work the behaviour of hydrogenated foils after charging is accompained by scanning electron microscopy (SEM) and X-ray diffraction. The scanning electron microscopy is succesfully used to distinguish the two phases (α-Ni and β-NiH_x) and to observe the cracks evolution during the hydride decomposition.

Materials and Methods

Thin foils (0.02mm thick) of high purity nickel were hydrogenated by electrolytic charging in a 1N H_2SO_4 solution with 20 mA/cm^2 by 24 hours. As_2O_3 was used as catalyst in a concentration of $5x10^{-5}$ mol/l. After the hydrogenation the samples were water cleaned, dryed and put into the microscope in less than five minutes. The SEM images were obtained in a JEOL 840 microscope operating in the backscattered mode. Time spaced pictures were taken from the same sample and sometimes the same area for 18 hours. Between two pictures the Faraday cup was introduced to preserve the sample. The hydrogenated samples were also analysed by X-ray diffraction immediately after the charging and during natural aging. The x=H/Ni ratio was calculated from the ΔV expansion of the unit cell [12]:

$$x = H / Ni = \frac{\Delta V}{4 \cdot 2.8} \qquad (1)$$

X-ray diffraction was carried out in a Siemens D-5000 diffractometer with Kα-Cu radiation. The sample was rotated during the measurement to minimize texture effects.

Results

Hydride decomposition

Figure 1 shows the X-ray diffractogram after hydrogenation (curve A) and after hydrogenation and 4 hours of aging (curve B). The α-Ni and β-NiH_x phases have lattice parameters 3.72Å and 3.58Å, respectively. The ratio x=H/Ni=0.68 of the β hydride is calculated from the unit cell expansion (equation 1). Figure 2 shows the exponential decrease of nickel hydride with time. The %$NiH_{0.68}$ was calculated from the X-ray diffraction patterns, taking into account only (200) and (111) reflections.

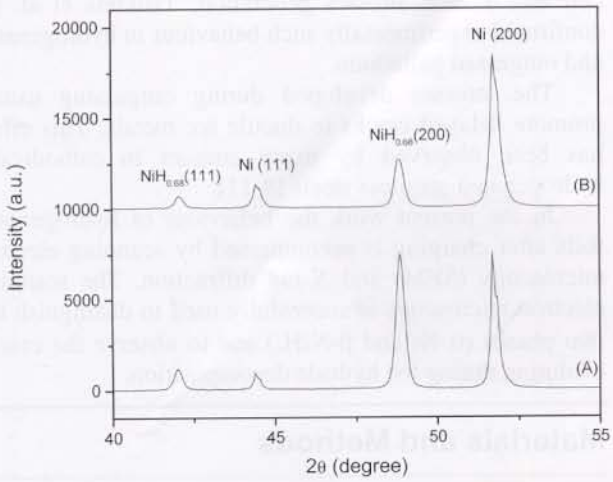

Fig.1: X-ray diffraction of hydrogenated nickel: (a) just after the electrolytic charging and (b) 4 hours after electrolytic charging (natural aging).

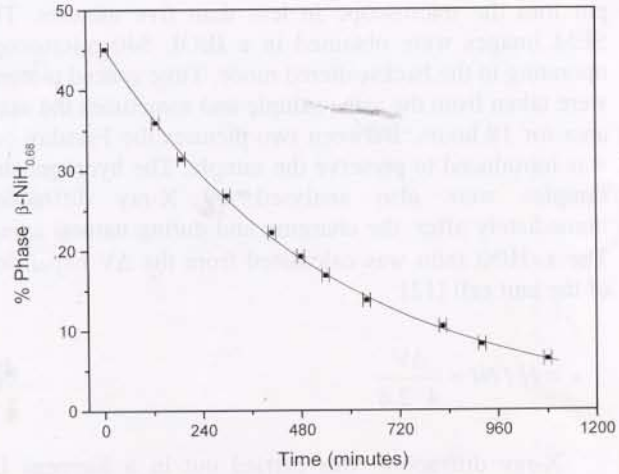

Fig.2: Exponential decay of the amount of β-$NiH_{0.68}$ during natural aging.

Figures 3 and 4 show the backscattered electrons image of samples as hydrogenated and as hydrogenated and aged for 4 hours, respectively. A contrast between the phases α-Ni and β-$NiH_{0.68}$ is observed. The α-Ni phase is clear and the β-$NiH_{0.68}$ hydride is grey that is due to the presence of light hydrogen atom. It is worth noticing that these two phases have never been distinguished by microscopy. In this field, Schober and Dieker [13] have applied Ag and Pd decoration techniques to observe local hydrogen in nickel surfaces.

The average atomic number of the α-Ni is Z_{Ni}=28 and that of the hydride β-$NiH_{0.68}$ is 17.1. The densities of α and β are 8.91 and 7.74 g/cm^3, respectively. These differences explain the contrast between the two phases obtained in the backscattered mode.

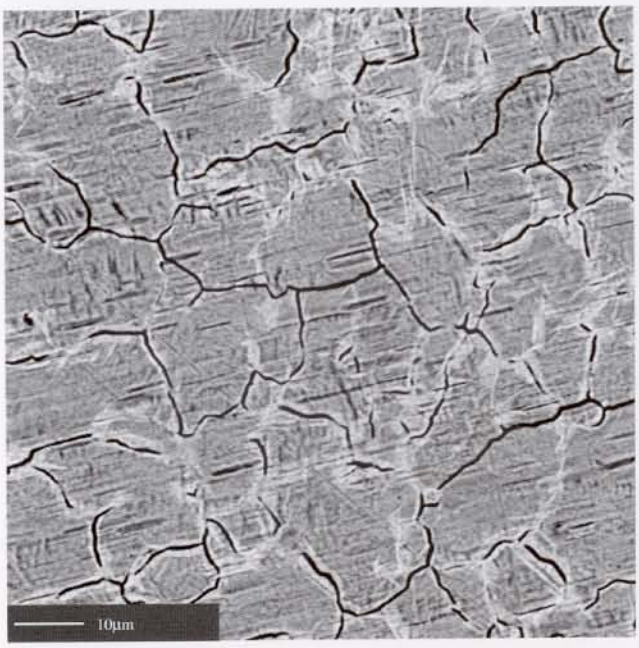

Fig.: 3: Backscattered electrons image of the nickel foil just after the hydrogenation.

The decrease of the amount of the β-$NiH_{0.68}$ with aging time, as evidenced by the X-ray diffraction analysis, can also be observed by SEM. It is possible that in the vacuum chamber of the microscope the rate of hydride decomposition is enhanced, as a simple application of the Le Chatelier's principle.

The decomposition of the hydride can be written as follows: $\beta(NiH_x) \rightarrow \alpha(Ni) + 0.5xH_2$. This reaction starts in the regions adjacent to the intergranular cracks (figure 3). Some details of figures 3 and 4 show that the α-Ni formed from the hydride may grows with an acicular morphology.

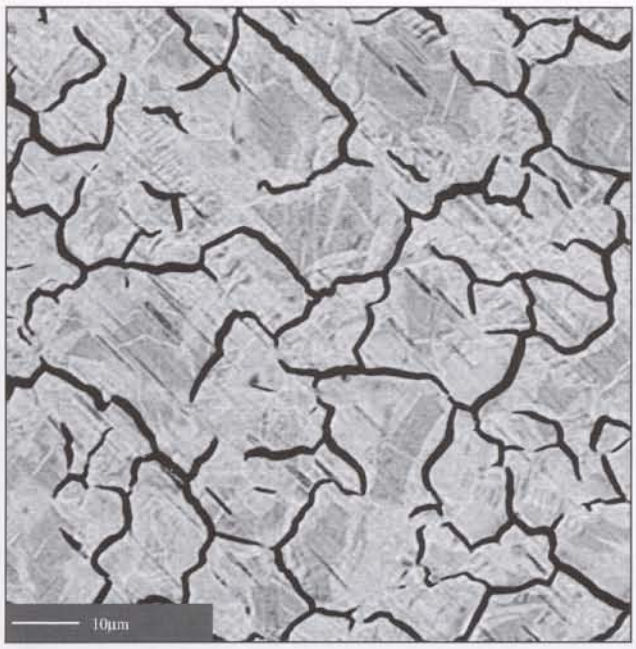

Fig.4: Backscattered electrons image of the nickel foil 4 hours after the hydrogenation (the sample was kept in vaccun into the microscope chamber).

Intergranular cracking

During the electrolytic hydrogenation at room temperature the hydrogen absorption and desorption may take place at the same time because of the high instability of the nickel hydride at room temperature. The β hydride formation occurs with lattice expansion and the H desorption promotes a contrary effect. As a result, tension and compression stresses are generated during the hydrogenation. The intergranular cracks observed in figure 3 are the manifestation of these stresses and also of the high susceptibility of nickel to hydrogen embrittlement. Accordingly to Yao et al. [1] pure nickel changes its fracture mode from transgranular to intergranualr when the hydrogen concentration at grain boundaries reaches a critical value of 6.5 to 9.8 at.%. The $NiH_{0.68}$ stoichiometry means an atomic concentration C_H=40.5at.%, i.e., more than four times the critical value.

When the intergranular crack is opened it becomes a preferential place for the hydride decomposition, as suggested by figure 3.

The sequence of figures 5, 6 and 7 shows the propagation and opening of the intergranular cracks in the same area, with the same magnification.

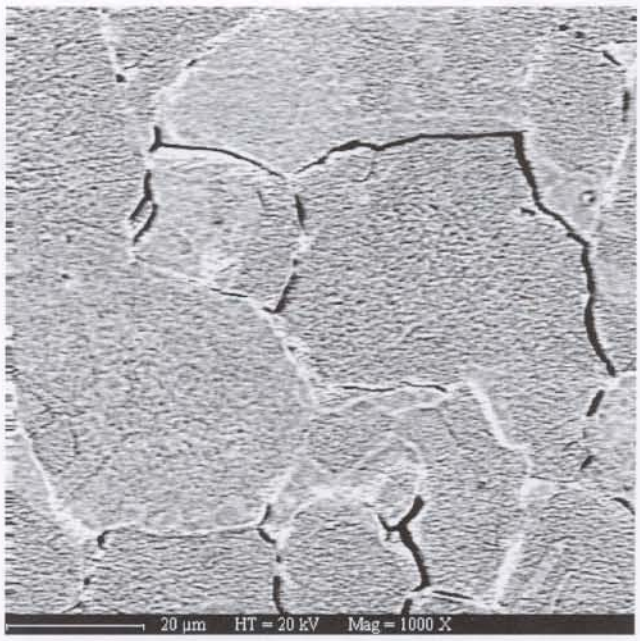

Fig. 5: Hydrogenated sample just after charging.

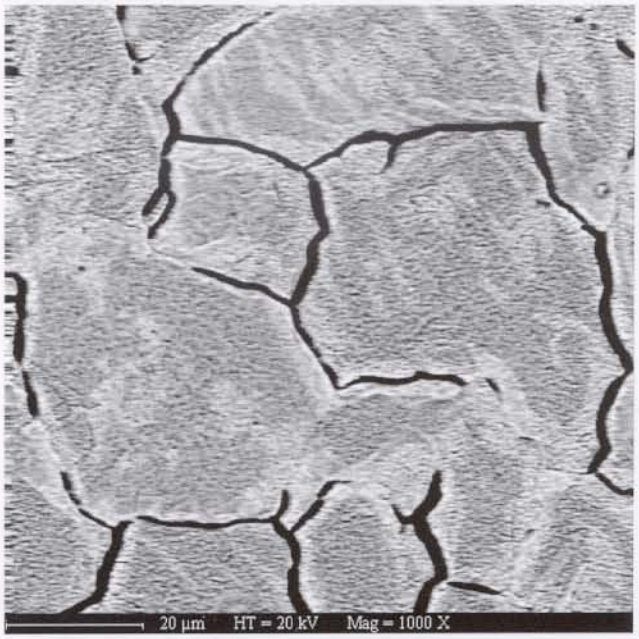

Fig. 6: Hydrogenated sample 2 hours after charging (same region of figure 5 to show the evolution of intergranular cracks).

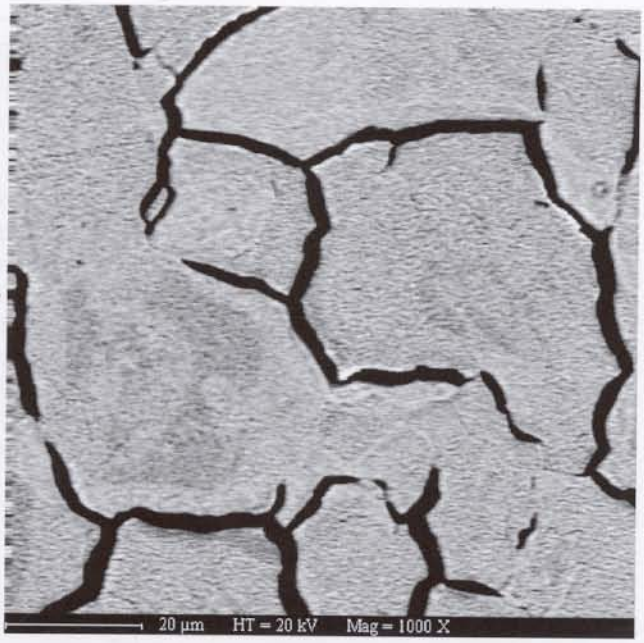

Fig. 7: Hydrogenated sample 18 hours after charging (same region of figures 5 and 6 to show the evolution of intergranular cracks).

The explanation for the crack opening and propagation lies in the stress field developed during the outgassing.The hydride decomposition is accompanied by lattice contraction that promotes mainly tension stresses. These stresses concentrate in the pre-existing cracks and makes them to open. This explains the increase of the average crack thickness that can be observed comparing figures 3 and 4. The dark parallell needles observed in figure 3 are due to the polishment, but some of them can become intragranular craks during the hydride decomposition (figure 4).

Discussion

The SEM characterization of nickel foils hydrogenated by electrolytic charging revealed the following features:

- The nickel hydride β-$NiH_{0.68}$ and the α-Ni phase could be distingued by backscattered electron image, due to the density or average atomic number differences.
- It was possible to observe the β-$NiH_{0.68}$ decomposition in situ.
- Intergranular cracks developed during the electrolytic charging propagate and become continuously larger during the natural aging, due to the tensile stresses developed during the hydrogen desorption.

Acknowledgments

S.S.M. Tavares would like to acknowledge CNPq (brazilian national research agency) for financial support (470385/01-4 NV).

References

1. Yao, J., Cahoon, J.R., Meguid, S. A., (1993) Metall. Trans. A, 24A, p.105-112.
2. Jing-Zhi Yu, Sun, Q., Wang, Q., Kawazoe, Y., (1999) Mat. Trans. JIM 4, p.1244-1248.
3. Fukai, Y., (1995) J. of Alloys and Comp. 231, p.35-42.
4. Hanson, M., Bauer, H.J., (1992) J. Alloys and Comp. 179, p.339-349.
5. Traverse, A., Kachnowski, T., Thomé, L., Bernas, H., (1980) Phys. Review B 22, p.4355-4365.
6. Wertheim, G.K., Buchanan, D.N.E. (1967) J. Phys. Chem. Solids 28, p.225-230.
7. Tsukuda, N., Itoh, K., Morioka, N., Ohkubo, H., Kuramoto, E., (1999) J. of Alloys and Comp. 293-295, p.174-177.
8. Herms, E., Olive, J.M., Puiggali, M., (1999) Mat. Sci. Eng. A272, p.279-283.
9. Yang, Q., Qiao, L. J., Chiovelli, S., Luo, J. L. (1999) Scripta Materiallia 40(11) p.1209-1214.
10. Mathias, H., Katz, Y., Nadiv, S., paper 2C11 in "Deuxième Congrès International L'hydrogen dans les métaux", Paris (1977).
11. Zakroczymski, T., Szklarska-Smialowska, Z., Smialowski, M., (1983) Corrosion 39, p.20.
12. Vargas, P., Christinsen, N. E. (1987) Physical Review B 35(4), p.1993-2004.
13. Schoeber, T., Dieker, C. (1983) Metallurgical Trans. A 14A, p.2440-2442.